

Two coupled Josephson junctions: dc voltage controlled by biharmonic current

L. Machura, J. Spiechowicz, M. Kostur, and J. Łuczka

Institute of Physics, University of Silesia, Katowice, Poland

E-mail: Jerzy.Luczka@us.edu.pl

Abstract. We study transport properties of two Josephson junctions coupled by an external shunt resistance. One of the junction (say, the first) is driven by an unbiased ac current consisting of two harmonics. The device can rectify the ac current yielding a dc voltage across the first junction. For some values of coupling strength, controlled by an external shunt resistance, a dc voltage across the second junction can be generated. By variation of system parameters like the relative phase or frequency of two harmonics, one can conveniently manipulate both voltages with high efficiency, e.g., changing the dc voltages across the first and second junctions from positive to negative values and *vice versa*.

PACS numbers: 05.60.-k, 74.50.+r, 85.25.Cp 05.40.-a,

1. Introduction

Transport phenomena in periodic structures by harvesting the unbiased external time-periodic stimuli and thermal equilibrium fluctuations have been one of the hottest topic in nowadays science. Examples range from biology and biophysics [1] to explain directed motion of biological motors [2] and particle transport in ion channels [3], or to design new separation techniques [4], to meso- and nano-physics covering newest and up-to-date experiments with optical lattices [5], persistent currents in quantum rings [6] and Josephson junctions [7], to mention only a few. The physics of the latter has been studied for almost five decades now [8]. Devices with Josephson junctions constitute a paradigm of nonlinear systems exhibiting many interesting phenomena in classical and quantum regimes. Yet new and interesting phenomena arise as researchers are able to use an advantage of powerful computer simulations followed by real experiments on junctions proving theoretically predicted findings [9, 10, 11]. In this paper we study a system of two coupled Josephson junctions driven by an external ac current having two harmonics. Such driving has been considered as a source of energy pumped into the system and as an agent transferring the system to non-equilibrium states. Transport phenomena in non-equilibrium states are of prominent interest from both theoretical and experimental point of view. For example, transport processes driven by biharmonic driving have been intensively studied in variety of systems and in various regimes. We can quote: Hamiltonian systems [13], systems in the overdamped regime [12, 14] and for moderate damping [15, 16], dissipative quantum systems [17], electronic quantum pumps [18] and quantum control of exciton states [19], cold atoms in the optical lattices [5, 20, 21], soliton physics [22] and driven Josephson junctions [23]. Here we intend to consider another aspect of transport in the system which consists of two coupled elements (subsystems). In particular, we take into consideration two coupled Josephson junctions. In a more general context it is a system which can be described by two degrees of freedom (it can consist of two interacting particles or one particle moving on a two-dimensional substrate) [24]. The question is: What new properties of transport can be induced by interaction between two elements and under what conditions can transport be generated in the second element if the driving is applied only to the first element.

The layout of the paper is as follows: In section 2, we detail the system of two Josephson junction coupled by an external shunt resistance. Next, in section 3, we specify external driving applied to one of the junctions. In section 4, we analyze generic properties of dc voltages across the first and second junctions. In section 5, we elaborate on the voltage control. Section 6 provides summary and conclusions.

2. Model and its dynamics

Let us consider a system of two coupled resistively shunted Josephson junctions. The equivalent circuit representation of the system is illustrated in figure 1. The junctions are

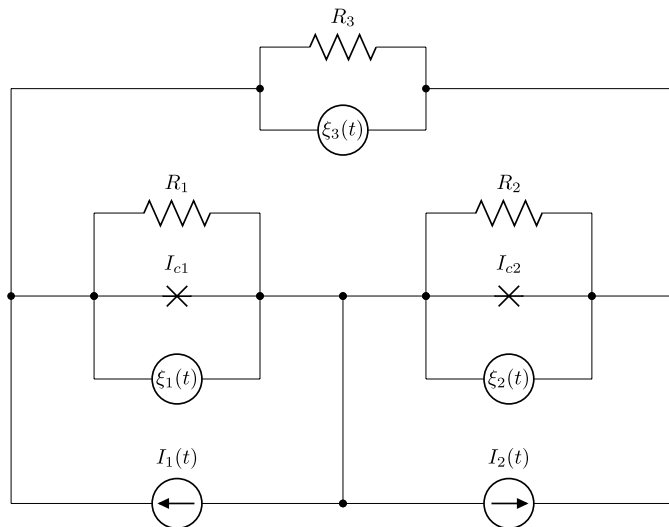


Figure 1. The system of two resistively shunted Josephson junctions coupled by an external shunt resistance R_3 and driven by the currents $I_1(t)$ and $I_2(t)$.

characterized by the critical currents (I_{c1}, I_{c2}), resistances (R_1, R_2) and phases (ϕ_1, ϕ_2) (more precisely, the phase differences of the Cooper pair wave functions across the junctions). The junctions are externally shunted by the resistance R_3 and driven by external currents $I_1(t)$ and $I_2(t)$. We also include into our considerations Johnson thermal noise sources $\xi_1(t), \xi_2(t)$ and $\xi_3(t)$ associated with the corresponding resistances R_1, R_2 and R_3 .

From the Kirchoff current and voltage laws, and two Josephson relations one can obtain the following equations

$$\begin{aligned} \frac{R}{R_1} \frac{\hbar}{2e} \dot{\phi}_1 &= (R_2 + R_3)[I_1(t) - I_{c1} \sin \phi_1] + R_2[I_2(t) - I_{c2} \sin \phi_2] \\ &\quad - (R_2 + R_3) \xi_1(t) - R_2 \xi_2(t) - R_3 \xi_3(t), \\ \frac{R}{R_2} \frac{\hbar}{2e} \dot{\phi}_2 &= (R_1 + R_3)[I_2(t) - I_{c2} \sin \phi_2] + R_1[I_1(t) - I_{c1} \sin \phi_1] \\ &\quad - (R_1 + R_3) \xi_2(t) - R_1 \xi_1(t) + R_3 \xi_3(t), \end{aligned} \quad (1)$$

where the dot denotes a derivative of $\phi_i = \phi_i(t)$ ($i = 1, 2$) with respect to time t and $R = R_1 + R_2 + R_3$. We assume that all resistors are at the same temperature T and the thermal equilibrium noise sources are represented by zero-mean Gaussian white noises $\xi_i(t)$ ($i = 1, 2, 3$) which are delta-correlated, i.e. $\langle \xi_i(t) \xi_j(s) \rangle \propto \delta_{ij} \delta(t - s)$ for $i, j \in \{1, 2, 3\}$. Note a symmetry property of equations (1) with respect to the change $R_1 \leftrightarrow R_2$.

The limitations of the model (1) and its range of validity are discussed e.g. in Ref. [25]. In particular, we work within the semi-classical regime of small junctions for which a spatial dependence of characteristics can be neglected, a displacement current accompanied with the junction capacitance is sufficiently small and can be ignored, and photon-assisted tunneling phenomena do not contribute.

The dimensionless variables and parameters can be introduced in various way. Here, we follow Ref. [26] and define the dimensionless time τ as:

$$\tau = \frac{2eV_0}{\hbar}t, \quad (2)$$

where

$$V_0 = I_c \frac{R_1(R_2 + R_3)}{R_1 + R_2 + R_3}, \quad I_c = \frac{I_{c1} + I_{c2}}{2} \quad (3)$$

are the the characteristic voltage and averaged critical current, respectively. The corresponding dimensionless form of equations (1) reads

$$\begin{aligned} \dot{\phi}_1 &= I_1(\tau) - I_{c1} \sin \phi_1 + \alpha[I_2(\tau) - I_{c2} \sin \phi_2] + \sqrt{D} \eta_1(\tau), \\ \dot{\phi}_2 &= \alpha\beta[I_2(\tau) - I_{c2} \sin \phi_2] + \alpha[I_1(\tau) - I_{c1} \sin \phi_1] + \sqrt{\alpha\beta D} \eta_2(\tau), \end{aligned} \quad (4)$$

where now the dot denotes a derivative with respect to dimensionless time τ and all dimensionless currents are in units of I_c . E.g., $I_{c1} \rightarrow I_{c1}/I_c$. The parameter

$$\alpha = \frac{R_2}{R_2 + R_3} \in [0, 1] \quad (5)$$

is the coupling constant between two junctions and can be controlled by the external resistance R_3 . The parameter $\beta = 1 + (R_3/R_1)$. The noises $\eta_1(\tau)$ and $\eta_2(\tau)$ are zero-mean δ -correlated Gaussian white noises, i.e. $\langle \eta_i(\tau)\eta_j(\tau') \rangle = \delta_{ij}\delta(\tau - \tau')$ for $i, j \in \{1, 2\}$ and are linear combinations of noises $\xi_i(t), i = 1, 2, 3$. The dimensionless noise strength is $D = 4ek_B T/\hbar\bar{I}_c$, where k_B is the Boltzmann constant.

Note that the dimensionless form (4) is not symmetrical with respect to the change $R_1 \leftrightarrow R_2$. It is because of the definition of the dimensionless time (2) which is extracted from the first equation of the set (1) and, in consequence, the asymmetry of V_0 in equation (3) with respect to R_1 and R_2 .

3. System driven by biharmonic current

The dynamic behavior of two Josephson junctions described by equations (4) is analogous to the overdamped dynamics of two interacting Brownian particles moving in spatially symmetric periodic structures and driven by external time-dependent forces. However, it is not a potential system. If we think of ϕ_1 and ϕ_2 as position coordinates of two particles, then $\dot{\phi}_1$ and $\dot{\phi}_2$ correspond to the velocity of the first and second particles, respectively. In this mechanical analogue, junction voltage is represented by particle velocity and time-dependent current $I_i(\tau)$ is represented by external force. We can use this analogue to visualize junction dynamics. The main transport characteristics of such mechanical systems are: the long-time averaged velocity $v_1 = \langle \dot{\phi}_1 \rangle$ of the first particle and the long-time averaged velocity $v_2 = \langle \dot{\phi}_2 \rangle$ of the second particle. The question is under what circumstances one can induce transport characterized by directed motion of both particles in the stationary regime, i.e. when $v_1 \neq 0$ and $v_2 \neq 0$. In terms of the Josephson junction system (4) it corresponds to the dimensionless long-time averaged dc voltages $v_1 = \langle \dot{\phi}_1 \rangle$ and $v_2 = \langle \dot{\phi}_2 \rangle$ across the first and second junction, respectively.

Transport in symmetric periodic systems like (4) can be trivially induced by biased external drivings $I_1(\tau)$ or/and $I_2(\tau)$. A non-trivial case is when zero-mean (non-biased) driving can induce transport. An example of zero-mean driving is the simplest harmonic signal $I(\tau) = A \cos(\omega\tau)$. From the symmetry property of equations (4) it follows that such a current source is unable to induce non-zero averaged voltages, for details see [14, 16, 21, 27, 28, 29]. However, when the system is driven by external currents having two harmonics, i.e. when [30]

$$I_i(\tau) = A_i [\cos(\omega_i\tau) + \varepsilon_i \cos(\Omega_i\tau + \theta_i)], \quad i = 1, 2, \tag{6}$$

then transport can be induced within tailored parameter regimes.

In the paper, we will study a particular case when the biharmonic ac current (6) is

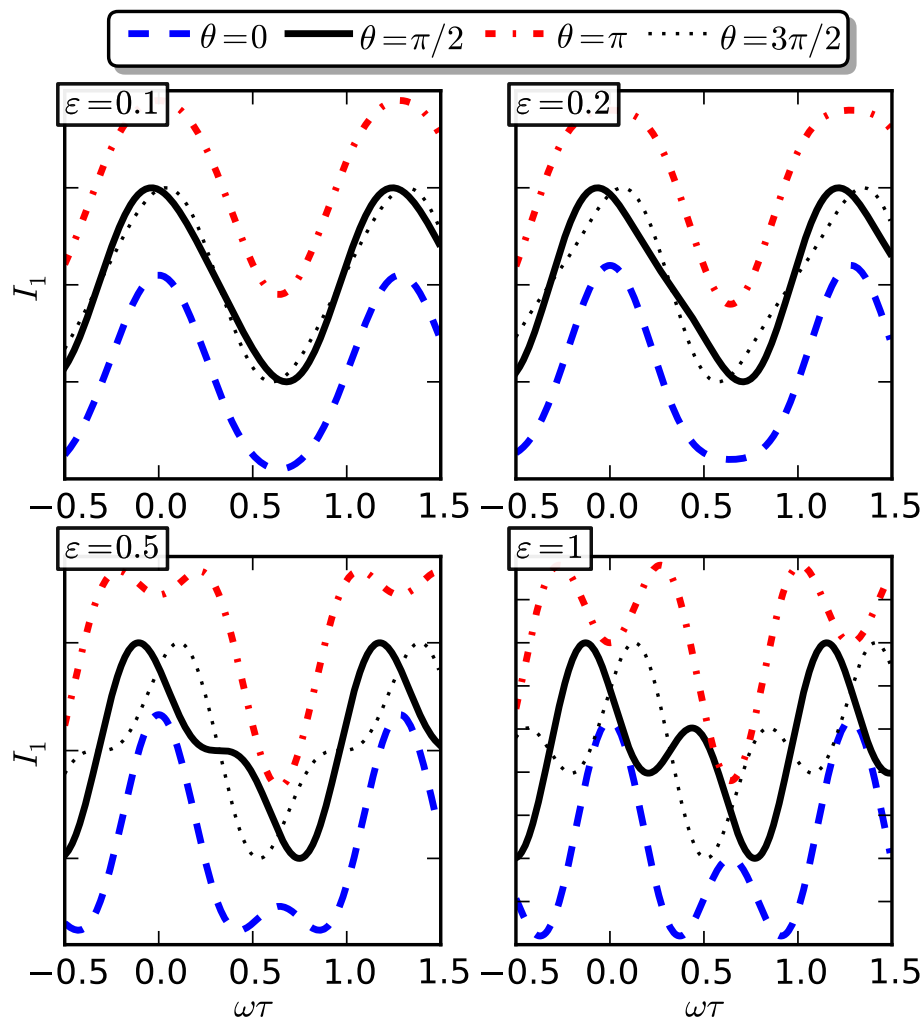


Figure 2. (color online). Illustration of the biharmonic current (7) for $a_1 = 1$ and selected values of other parameters. Only symmetric ($\theta = 0, \pi$) and antisymmetric ($\theta = \pi/2, 3\pi/2$) forms of the current are displayed for specific values of the relative phase θ . For clarity, the curves are offset vertically from one another to facilitate comparison.

applied only to one (say, the first) junction, and has the form

$$I_1(\tau) = a_1 [\cos(\omega\tau) + \varepsilon_1 \cos(2\omega\tau + \theta)], \quad I_2(\tau) = 0. \quad (7)$$

It is known that without coupling to the second junction (i.e. when $\alpha = 0$), the averaged dc voltage v_2 across the second junction is zero while the dc voltage v_1 across the first junction is non-zero in some regions of the parameters space. We can formulate several fundamental questions: (a) What is the influence of coupling α on the voltage v_1 ? (b) Can the voltage across the second junction be induced by coupling (5) and how it depends on its strength? (c) Can the voltages reversal be obtained by changing the control parameters? (d) Can the voltages v_1 and v_2 have opposite signs? Properties of the ac current $I_1(\tau)$ determine whether the voltages v_1 and v_2 display the above mentioned features. One can distinguish two special cases of the two-harmonics ac current $I_1(\tau)$:

(i) The first case is when there is such τ_0 that $I_1(\tau_0 + \tau) = I_1(\tau_0 - \tau)$. It means that the driving is symmetric or invariant under the time-inversion transformation. It is the case when $\theta = \{0, \pi\}$, see dashed and dotted-dashed lines in figure 2.

(ii) The second case is when there is such τ_1 that $I_1(\tau_1 + \tau) = -I_1(\tau_1 - \tau)$. This is the case of the antisymmetric driving realized for the phases $\theta = \{\pi/2, 3\pi/2\}$, see solid and dotted lines in figure 2.

The analysis of a similar system biased by a dc current and driven by an unbiased harmonic ac signal has been recently presented in Ref. [31]. The main difference between these two set-ups is a constant dc current which in turn may lead to the phenomenon of the negative mobility (resistance) [9]. Here, there is no such constant current applied to the system. However, by applying asymmetric ac signals we hope to be able to control the behavior of the first and second junctions. We would like to convince reader that transport across the junction can be qualitatively controlled just by adjusting the *shape* of the external signal applied to *one junction only*.

4. Voltage response to biharmonic current

To reduce a number of parameters of the model, we consider a special case of two *identical* junctions. In such a case $I_{c1} = I_{c2} = 1, R_1 = R_2, \alpha\beta = 1$ and equations (4) take the form

$$\begin{aligned} \dot{\phi}_1 &= I_1(\tau) - \sin \phi_1 - \alpha \sin \phi_2 + \sqrt{D} \xi'(\tau), \\ \dot{\phi}_2 &= -\sin \phi_2 + \alpha [I_1(\tau) - \sin \phi_1] + \sqrt{D} \xi''(\tau), \end{aligned} \quad (8)$$

where the driving current $I_1(\tau) = I_1(\tau; a_1, \varepsilon_1, \theta)$ is given by the relation (7).

Now, we make four general conclusions about the dc voltages as a consequence of the symmetry properties of the ac driving current $I_1(\tau)$:

(A) – Let us consider the voltages $v_1 = v_1(\varepsilon_1)$ and $v_2 = v_2(\varepsilon_1)$ as functions of the amplitude ε_1 of the second harmonic. If we make the transformation $\varepsilon_1 \rightarrow -\varepsilon_1$ to equations (8), then it follows that

$$v_1(-\varepsilon_1) = -v_1(\varepsilon_1), \quad v_2(-\varepsilon_1) = -v_2(\varepsilon_1). \quad (9)$$

These relations yield $v_1(0) = -v_1(0), v_2(0) = -v_2(0)$ and we conclude that $v_1(0) = 0$ and $v_2(0) = 0$ when the second harmonic is zero, i.e. when $\varepsilon_1 = 0$.

(B) – The sign of voltages $v_1 = v_1(\theta)$ and $v_2 = v_2(\theta)$ can be controlled by the phase θ . Indeed, if one changes the phase $\theta \rightarrow \theta \pm \pi$ then $\varepsilon_1 \cos(2\omega\tau + \theta \pm \pi) \rightarrow -\varepsilon_1 \cos(2\omega\tau + \theta)$ and from the relations (9) one gets

$$v_1(\theta \pm \pi) = -v_1(\theta), \quad v_2(\theta \pm \pi) = -v_2(\theta). \quad (10)$$

(C) – Because the driving $I_1(\tau)$ is the same for $\theta \rightarrow \pi - \theta$ and for $\theta \rightarrow \pi + \theta$, the symmetry relations

$$v_1(\pi - \theta) = v_1(\pi + \theta), \quad v_2(\pi - \theta) = v_2(\pi + \theta) \quad (11)$$

hold for any value of the phase θ .

(D) – For the antisymmetric ac current, equations (8) are invariant under the time reversal transformation $t \rightarrow -t$. As a consequence [14, 21, 28]

$$v_1(\pi/2) = v_1(3\pi/2) = 0, \quad v_2(\pi/2) = v_2(3\pi/2) = 0. \quad (12)$$

The above set of equations (8) cannot be handled by standard analytical methods used in ordinary differential equations. Therefore we have carried out comprehensive numerical simulations. We have employed Stochastic Runge–Kutta algorithm of the 2nd order with the time step of $[10^{-3} \div 10^{-4}](2\pi/\omega)$. We have chosen initial phases $\phi_1(0)$ and $\phi_2(0)$ equally distributed over one period $[0, 2\pi]$. Averaging was performed over $10^3 - 10^6$ different realizations and over one period of the external driving $2\pi/\omega$. All numerical calculations have been performed using CUDA environment on desktop computing processor NVIDIA GeForce GTX 285. This gave us a possibility to speed the numerical calculations up to few hundreds times more than on typical modern CPUs [32].

We begin the analysis of transport properties of the system (8) by some general comments about its long-time behavior. In the long time limit, the averaged voltages $\langle \dot{\phi}_i(\tau) \rangle$ can be presented in the form of a series of all possible harmonics, namely,

$$\lim_{\tau \rightarrow \infty} \langle \dot{\phi}_i(\tau) \rangle = v_i + \sum_{n=1}^{\infty} v_i(n\omega\tau), \quad i = 1, 2, \quad (13)$$

where v_i is a dc (time-independent) component and $v_i(n\omega t)$ are time-periodic functions of zero average over a basic period.

When both a_1 and ε_1 are small, the dc components v_1 and v_2 of averaged voltages are zero in the long time limit. It can be inferred from the structure of equations (8): at least one of the amplitudes of the driving current $I_1(\tau)$ should be greater than the amplitude $I_{c1} = 1$ of the Josephson supercurrent. Also for high frequency ω , the averaged dc voltages are zero: very fast positive and negative changes of the driving current cannot induce the dc voltage and only multi-harmonic components of the voltages can survive. For smaller values of the frequency and higher values of amplitude, one can observe a stripe-like structure of non-zero values of both voltages v_1 and v_2 .

We can identify four remarkable and distinct parameter regimes where:

(I) $v_1 > 0$ and $v_2 > 0$,

- (II) $v_1 < 0$ and $v_2 < 0$,
- (III) $v_1 < 0$ and $v_2 > 0$,
- (IV) $v_1 > 0$ and $v_2 < 0$.

The regimes (I) and (II) dominate in the parameter space. If the regime (I) is detected then the regime (II) can be obtained from the relations (10) by changing the relative phase θ of the biharmonic current $I_1(\tau)$. Likewise, if the regime (III) is found then the regime (IV) can be determined from the relations (10).

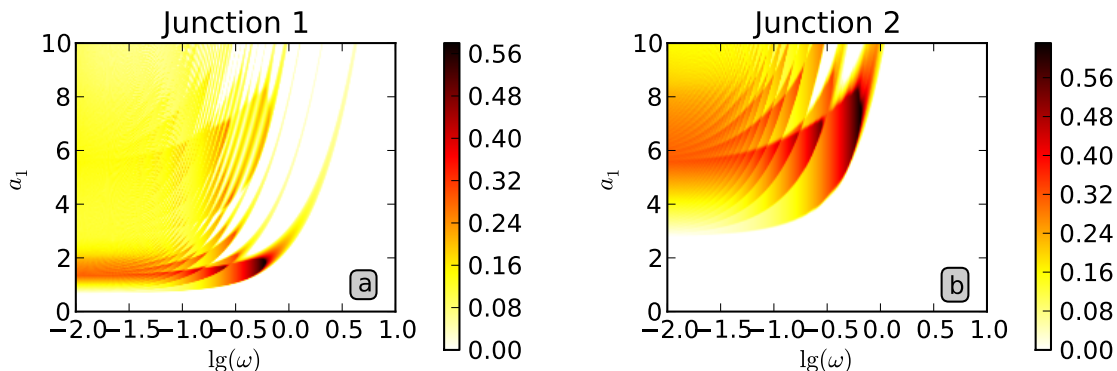


Figure 3. (color online). Transport properties of the system of two Josephson junctions driven by the ac current acting on the first junction. In panels a and b averaged dc voltages v_1 and v_2 across the first and second junction are shown for the coupling constant $\alpha = 0.25$, temperature $D = 0.001$, relative amplitude of the second harmonic $\varepsilon_1 = 0.5$ and the relative phase $\theta = 0$.

4.1. Dominated regime: the same sign of dc voltages v_1 and v_2

In figure 3 we present the regime (I) in the parameter plane $\{a_1, \omega\}$ which illustrate how voltages v_1 and v_2 depend on the amplitude a_1 and frequency ω of the biharmonic current $I_1(\tau)$ when other parameters are fixed. In this regime, both voltages always take non-negative values.

The dependence of voltages v_1 and v_2 on the current amplitude a_1 is depicted in panels (a) and (b) of figure 4. We observe that for smaller amplitudes of external ac current the transport is activated only on the first junction while the voltage across the second junction is zero. We can identify non-zero response of the first junction at the amplitude around $a_1 = 1$. The second junction awakes for larger values of amplitudes (the threshold is a little bit less than $a_1 = 4$). One can note non-monotonic behavior of all presented curves. After initial burst the amplitude of the voltage of the first junction decreases, revealing next enhancement together with the appearance of the non-zero voltage excited on the second junction (green dashed lines). For larger amplitude of the ac driving, voltages of both junctions decrease. In panels (a) and (b) of this figure, the phase θ of the second harmonic of the external signal is different: $\theta = 0$ in panel (a) and $\theta = \pi/3$ in panel (b). The inspection of the results reveals that the change of the phase from $\theta = 0$ to $\theta = \pi/3$ reduces the dc voltages more than twice.

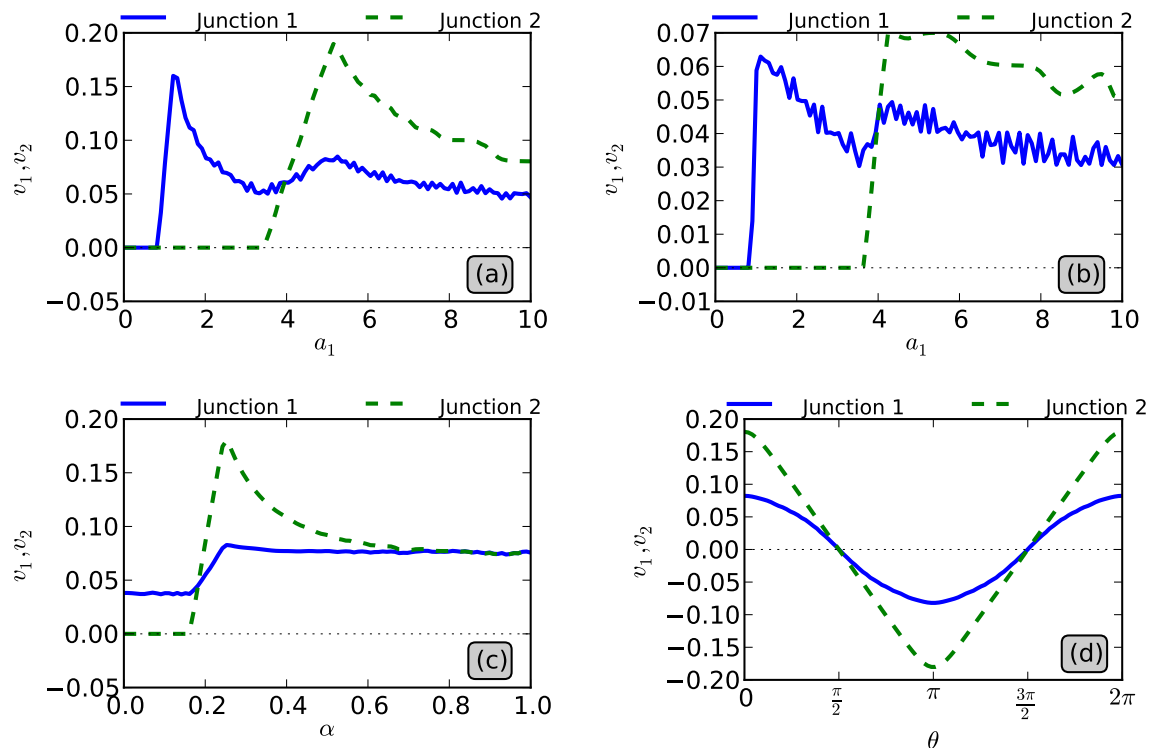


Figure 4. (color online). The stationary averaged dc voltages v_1 and v_2 across the first (blue solid line) and second (green dashed line) junction, respectively. The parameters are: the dimensionless temperature $D = 0.01$, the frequency $\omega = 0.01$ and strength of the second harmonic $\varepsilon_1 = 0.2$. The dependence on the external ac current amplitude a_1 is presented in panels: (a) for the relative phase $\theta = 0$ and (b) for $\theta = \pi/3$, and fixed coupling constant $\alpha = 0.25$. In panel (c) the dependence of voltages on the coupling constant α is depicted for fixed amplitude $a_1 = 5.15$ and phase $\theta = 0$. In panel (d) the role of the driving current symmetry controlled by the phase θ is shown for $a = 5.15$ and $\alpha = 0.25$.

In panel (c) of figure 4, the role of coupling is illustrated: for small values of the coupling constant α the voltage v_2 is zero. There is a threshold value α_c of coupling above which the voltage across the second junction can be generated. In the regime presented in figure 4, the threshold value $\alpha_c \approx 0.152$. From equation (5) it follows that the external shunt resistance R_3 can be a good control parameter which decides whether v_2 takes non-zero or zero values. For fixed remaining system parameters, one can induce non-zero voltage across the second junction by decreasing the resistance R_3 to values $R_3 < R_c = (\alpha_c^{-1} - 1)R_2$. For $R_3 > R_c$ the voltage v_2 diminishes.

In panel (d) of figure 4, the influence of the relative phase θ of two harmonic signals on the dc voltages is depicted. It is a numerical evidence for our consideration on symmetry relations (9)-(12). We can deduce two conclusions:

- (i) The maximal absolute values of voltages v_1 and v_2 are generated by the *symmetric* ac current, i.e. when $\theta = 0$ or π ;
- (ii) Both dc voltages v_1 and v_2 are zero when the ac current is *antisymmetric*, i.e. when

$\theta = \pi/2$ or $3\pi/2$.

From Refs [14, 28] it follows that for small amplitudes of both harmonics of the driving current (7) the dc voltages depend on the phase as $v_i \propto \cos \theta$ ($i = 1, 2$). Such a behavior is universal and does not depend on details of systems or models. E.g. it has been observed in transport of flux quanta in superconducting films, see panel (b) in figure 1 of Ref. [33].

As follows from equations (10), the regime (II) can be obtained from the regime (I) by change of the phase $\theta \rightarrow \theta \pm \pi$. Then the corresponding figures can be obtained from figures 3 and 4 by the reflection with respect to the horizontal axis. Therefore we do not discuss this regime and we do not show corresponding figures.

4.2. Regime of the opposite sign of dc voltages v_1 and v_2

Now, we address the question of whether we can identify parameter regimes (III) and (IV) where the dc voltages v_1 and v_2 take opposite sign. An illustrative example of such a regime is depicted in figure 5. We can identify a fine stripe-like structure of regions of non-zero dc voltages sparsely distributed in the parameter space. Outside the stripes, in large regions of parameter space, the voltages v_1 and v_2 are negligible small or zero.

The inspection of figures 5 suggests to perform a more accurate search for the horizontal section $a_1 = \text{const.}$ and the vertical section $\omega = \text{const.}$. In panels (a) and (b) of figure 6 we present results for the section $a_1 = 3$. One can note the unique feature of the occurrence of windows of the frequency ω where the voltage v_2 takes the opposite sign to the voltage v_1 . The voltages as a function of ω display the non-monotonic dependence exhibiting maxima and minima. We can detect the interval where absolute values of voltages operate synchronously: simultaneous increase and decrease both of them. For higher temperature $D = 10^{-2}$ and within the presented range of the base frequency ω the voltages across both junctions alternate showing very interesting and rare curves of opposite voltage reversals [34]. However, if we consider ten times lower temperature, i.e. $D = 10^{-3}$, then only one window of the states working contrariwise survives. It means that other windows are created by thermal equilibrium fluctuations.

Two panels (c) and (d) in figure 6 illustrate the section $\omega = 0.1139$ and the section $\omega = 0.1288$ to show the influence of the amplitude a_1 of the ac driving. The voltages as a function of a_1 are non-monotonic and local maxima and minima can be detected.

The influence of the relative amplitude ε_1 of the second harmonic is depicted in figure 7 for two values of the driving frequency $\omega = 0.1139$ (a) and $\omega = 0.1288$ (b). In the vicinity of $\varepsilon_1 = 0.1$ we can notice previous findings where the voltages have the opposite sign for both junctions. However, if we increase ε_1 then both voltages diminish and next take negative values following by positive signs for large ε_1 , see panel (a) for details. For faster current $\omega = 0.1288$ the situation is opposite - for larger ε_1 voltages become positive, next negative and end up with locked state for relatively large ε_1 . It is worth to mention that $\varepsilon_1 = 0$ relates to the situation where the second harmonic is zero resulting in a pure symmetric driving with no possible net transport. On the other

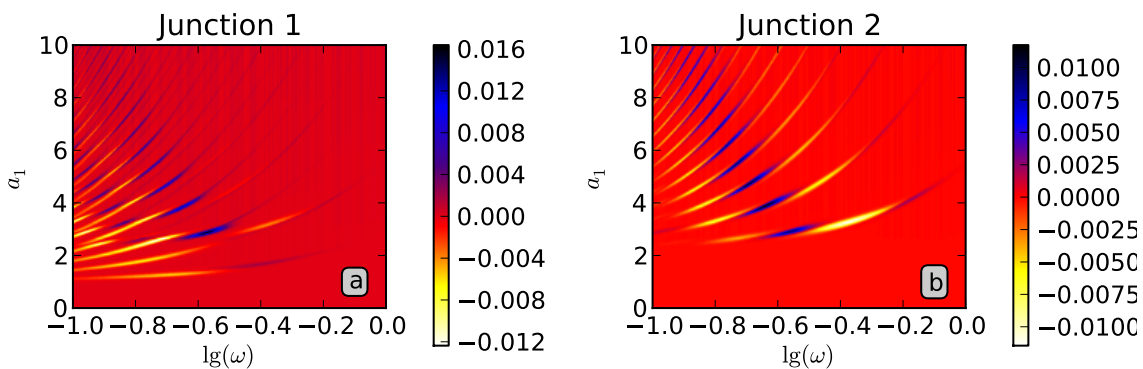


Figure 5. (color online). Transport properties of the system of two Josephson junctions driven by the ac current acting on the first junction. In panels a and b dc voltages v_1 and v_2 are shown for the parameters set $\alpha = 0.25$, $D = 0.01$, $\varepsilon_1 = 0.1$ and $\theta = \pi/2$ revealing the most interesting response of junctions with characteristic stripe-like structure of regions of non-zero dc voltages.

hand, if $\varepsilon_1 = 1$ then both harmonics of the signal (7) are equally strong and we are not able to say which part of it influences the dynamics of junctions more effectively.

In panel (c) we show the influence of interaction between two junctions on the voltage characteristics. The first observation is that there are optimal values of the coupling strength α for which absolute values of voltages are locally maximal. The second observation is that variation of the coupling strength can lead to the phenomenon of the voltage reversal [34]: the voltage changes its values from positive (negative) values to negative (positive) ones. The third observation is the same as presented in panel (c) of figure 4: there is a threshold value of coupling $\alpha = \alpha_c$ (or the resistance $R_3 = R_c$) such that for $\alpha < \alpha_c$ (or for $R_3 > R_c$) the voltage v_2 is reduced to zero.

In panel (d) we depict the influence of temperature. Most remarkably, transport is solely induced by thermal noise. Indeed, in the deterministic case (i.e. for $D = 0$), when no thermal fluctuations act, the dc voltages vanish. With increasing temperature, the voltage v_1 starts to increase to positive-valued local maximum. Next, it decreases crossing zero and reaches a negative-valued local minimum. For further increase of temperature, the voltage v_1 tends to zero. In turn, the voltage v_2 takes negative values reaching minimal value as temperature start to increase. Next, it increases crossing zero and reaches local maximum. Finally, it monotonically decreases toward zero. We observe that optimal temperature occurs at which the voltage v_1 is maximal. There is also another optimal temperature at which in turn the absolute value of v_2 is maximal. Moreover, one can identify the voltage reversal phenomenon: the both voltages change their sign as temperature is varied.

From the presented analysis it follows that a biharmonic drive allows one to conveniently manipulate transport with high efficiency by changing the system parameters.

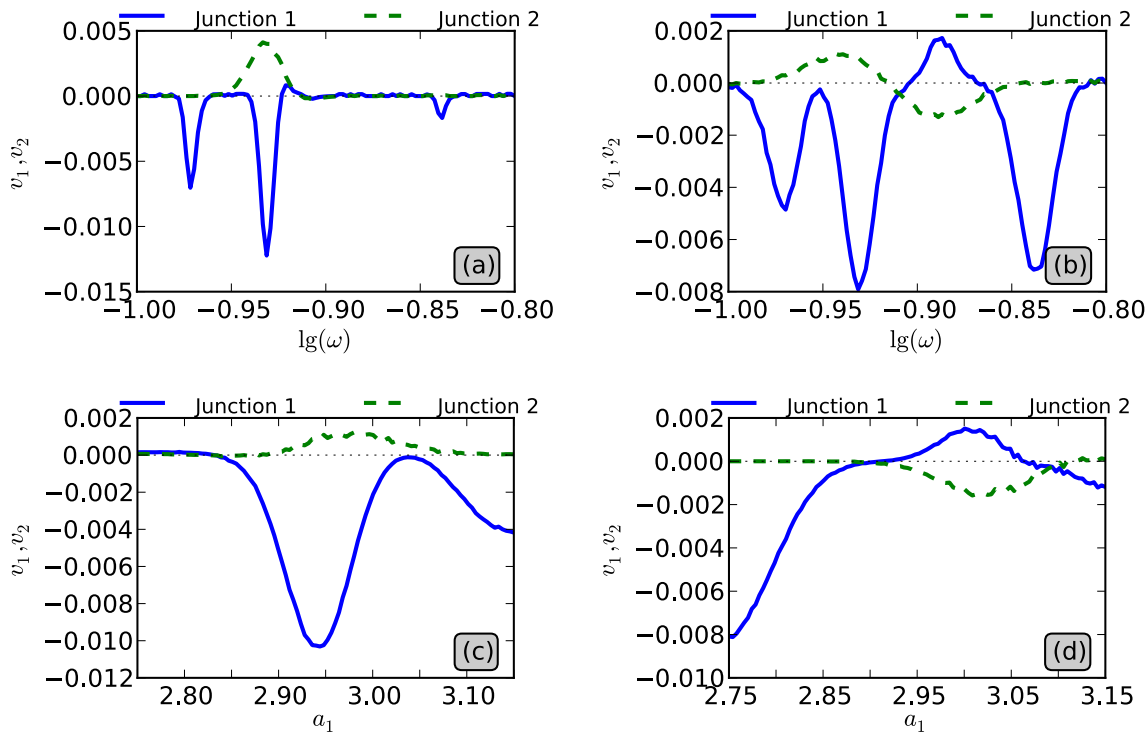


Figure 6. (color online). The stationary averaged dc voltages v_1 and v_2 across the first (blue solid line) and second (green dashed line) junction, respectively. The dependence on the frequency ω of the ac driving is presented in panels (a) and (b) at a fixed amplitude $a_1 = 3.0$. The temperature read $D = 10^{-3}$ on panel (a) and 10^{-2} on panel (b). In two lower panels (c) and (d) the dependence on the external ac current amplitude a_1 is presented at fixed frequency $\omega = 0.1139$ (c) and $\omega = 0.1288$ (d) for temperature $D = 10^{-2}$. Parameters used in all panels are: the coupling constant $\alpha = 0.5$, the relative amplitude of the second harmonic $\varepsilon_1 = 0.1$ and the relative phase $\theta = \pi/2$.

5. Summary

This paper presents the detailed study of the system of two coupled noisy Josephson junctions which undergoes the influence of the external ac biharmonic current applied to one of the junctions only. The dependence of voltages across the first and second junctions upon ac driving exhibits a rich diversity of transport characteristics. In particular, it is possible to control both junctions to operate simultaneously with positive or negative voltages of the same sign or, more interestingly, with the opposite sign. Moreover, the phenomenon of the voltage reversals is revealed: the voltages change the sign as one of the parameters is varied. Our findings can be experimentally verified in an accessible set-up of two Josephson junctions coupled by an external resistance. The work can open the perspective of a new type of electronic elements which is tunable between positive and negative dc voltages via external control parameters like the amplitudes and relative phases of an ac current. The straightforward extension of the ideas presented

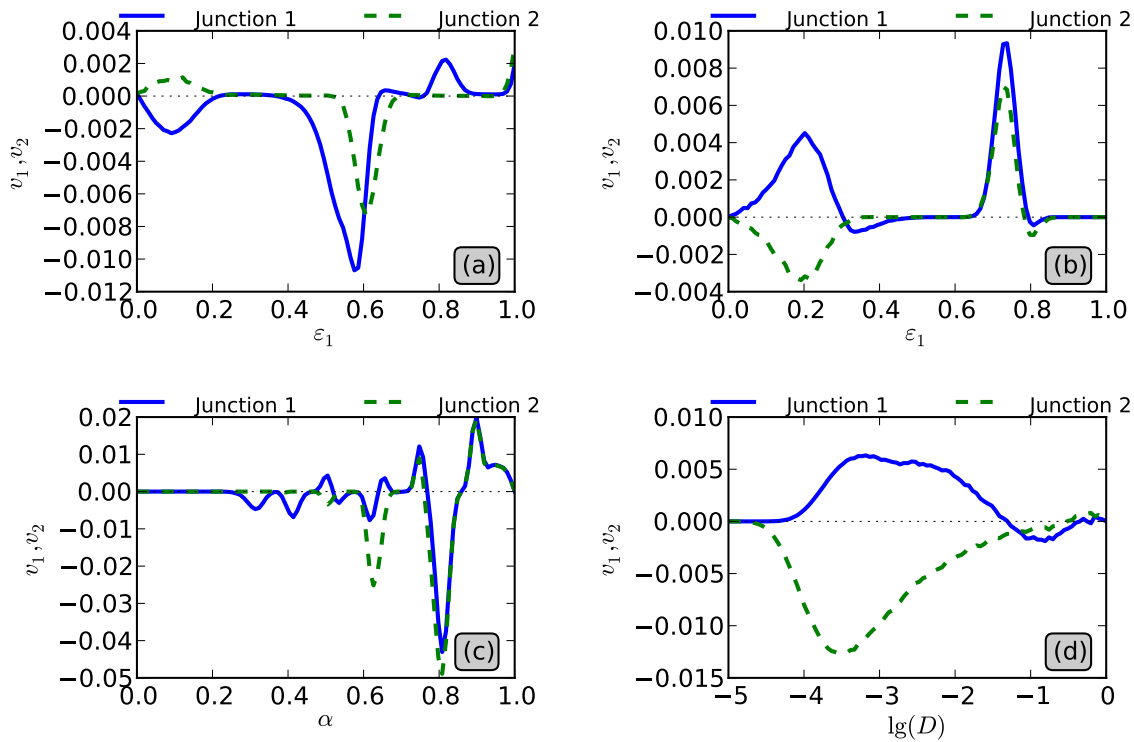


Figure 7. (color online). The stationary averaged voltages v_1 and v_2 across the first (blue solid line) and second (green dashed line) junction, respectively. The dependence on the relative amplitude ε_1 of the second harmonic of the ac driving is presented in panels (a) and (b) for fixed coupling $\alpha = 0.5$ and for two frequencies $\omega = 0.1139$ (a) and $\omega = 0.1288$ (b). In panel (c) the dependence of voltages on the coupling constant α is depicted for $\varepsilon_1 = 0.2$ and $\omega = 0.12884$. In panel (d) the role of temperature controlled by the dimensionless parameter D is shown for $\varepsilon_1 = 0.2$, $\omega = 0.1288$ and $\alpha = 0.5$. Parameters used in all panels read: relative phase $\theta = \pi/2$ and amplitude $a_1 = 3.0$. In panels (a)-(c) temperature $D = 10^{-2}$.

here would cover an increasing number of coupled junctions to three (or more) as well as study of other types of driving.

Acknowledgments

The work supported in part by the grant N202 052940.

References

- [1] Neimann A, Hänggi P, Jung P and Schimansky-Geier L 2004 *Noise in Biophysical Systems* (eds., Special Issue: *Fluctuation Noise Letters*, vol. 4, no. 1) p 1
- [2] Astumian R D 2002 *Sci. Am.* **285** 56
Astumian R D and Hänggi P 2002 *Phys. Today* **55** 33
- [3] Burada P S, Schmid G, Talkner P, Hänggi P, Reguera D and Rubi J M 2008 *Biosystems* **93** 16
- [4] Regtmeier J, Eichhorn R, Duong T T, Reimann P, Anselmetti P and Ros A 2007 *Eur. Phys. J. E* **22** 335

- [5] Jones P H, Goonasekera M and Renzoni F 2004 *Phys. Rev. Lett.* **93** 073904
Gommers R, Bergamini S and Renzoni F 2005 *Phys. Rev. Lett.* **95** 073003
Renzoni F 2005 *Cont. Phys.* **46** 161
- [6] Bluhm H, Koshnick N C, Bert J A, Huber M E and Moler K A 2009 *Phys. Rev. Lett.* **102** 136802
Machura L, Rogoziński S and Łuczka J 2010 *J. Phys.: Condens. Matter* **22** 422201
- [7] Barone A and Paternò G 1982 *Physics and Application of the Josephson Effect*, (New York: Wiley)
- [8] Josephson B D 1964 *Rev. Mod. Phys.* **36** 216.
- [9] Machura L, Kostur M, Talkner P, Łuczka J and Hänggi P 2007 *Phys. Rev. Lett.* **98** 040601
Kostur M, Machura L, Hänggi P, Łuczka J and Talkner P 2006 *Physica A* **371** 20
- [10] Machura L, Kostur M, Talkner P, Hänggi P and Łuczka J 2010 *Phys. E* **42** 590
Kostur M, Machura L, Talkner P, Hänggi P and Łuczka J 2008 *Phys. Rev. B* **77** 104509
Kostur M, Machura L, Łuczka J, Talkner P and Hänggi P 2008 *Acta Physica Polonica B* **39** 1115
- [11] Nagel J, Speer D, Gaber T, Sterck A, Eichhorn R, Reimann P, Ilin K, Siegel M, Koelle D, Kleiner R 2008 *Phys. Rev. Lett.* **100** 217001
- [12] Marchesoni F 1986 *Phys. Lett. A* **119** 221
Borromeo M and Marchesoni F 2005 *Europhys. Lett.* **72** 362
Borromeo M, Hänggi P and Marchesoni F 2005 *J. Phys.: Condens. Matter* **17** S3709
Borromeo M and Marchesoni F 2006 *Phys. Rev. E* **73** 016142
Chenggui Yao, Yan Liu and Meng Zhan 2011 *Phys. Rev. E* **83** 061122
- [13] Flach S, Yevtushenko O and Zolotaryuk Y 2000 *Phys. Rev. Lett.* **84** 2358
- [14] Yevtushenko O, Flach S, Zolotaryuk Y and Ovchinnikov A A 2001 *Europhys. Lett.* **54** 141
- [15] Wonneberger W and Breymayer H J 1981 *Z. Phys. B - Condensed Matter* **43** 329
Breymayer H J 1984 *Appl. Phys. A* **33** 1
- [16] Machura L, Kostur M and Łuczka J 2010 *Chemical Physics* **375** 445
Machura L and Łuczka J 2010 *Phys. Rev. E* **82** 031133
Cubero D, Lebedev V and Renzoni F 2010 *Phys. Rev. E* **82** 041116
- [17] Goychuk I and Hänggi P 1998 *Europhys. Lett.* **43** 503
- [18] Arrachea L 2007 *Physica B* **398** 450
- [19] Basieva T I, Basiev T T, Dietler G, Pukhov K K and Sekatskii S K 2006 *Phys. Rev. B* **74** 165329
- [20] Brown M and Renzoni F 2008 *Phys. Rev. A* **77** 033405
- [21] Denisov S, Flach S and Hänggi P 2010 in *Nonlinearities in Periodic Structures and Metamaterials*, (C. Denz, S. Flach, and Y. Kivshar, eds. *Springer Series in Optical Sciences* vol. 150) p 181 (Springer)
- [22] Salerno M and Zolotaryuk Y 2002 *Phys. Rev. E* **65** 056603
Müller P, Mertens F G and Bishop A R 2009 *Phys. Rev. E* **79** 016207
Rietmann M, Carretero-González R and Chacón R 2011 *Phys. Rev. A* **83** 053617
- [23] Monaco R 1990 *J. Appl. Phys.* **68** 679
Salerno M 1991 *Phys. Rev. B* **44** 2720
Filatrella G and Rotoli G 1994 *Phys. Rev. B* **50** 12802
Ustinov A V, Coqui C, Kemp A, Zolotaryuk Y and Salerno M 2004 *Phys. Rev. Lett.* **93** 087001
- [24] Reichhardt C, Olson C J and Hastings M B 2002 *Phys. Rev. Lett.* **89** 024101
Guantes R and Miret-Artés S 2003 *Phys. Rev. E* **67** 046212
Romero A H, Lacasta A M and Sancho J M 2004 *Phys. Rev. E* **69** 051105
Heinsalu E, Patriarca M and Marchesoni F 2008 *Phys. Rev. E* **77** 021129
Speer D, Eichhorn R and Reimann P 2009 *Phys. Rev. Lett.* **102** 124101
- [25] Kautz R L 1996 *Rep. Prog. Phys.* **59** 935
- [26] Nerenberg M A H, Blackburn J A and Jillie D W 1980 *Phys. Rev. B* **21** 118
- [27] Neumann E and Pikovsky A 2002 *Eur. Phys. J. B* **26** 219
Chacón R and Quintero N R 2007 *BioSystems* **88** 308
- [28] Quintero N R, Cuesta J A and Alvarez-Nodarse R 2010 *Phys. Rev. E* **81** 030102R

- [29] Kolton A B and Renzoni F 2010 *Phys. Rev. A* **81** 013416 (and refs therein)
- [30] Skov C E and Pearlstein E 1964 *Rev. Sci. Instr.* **35** 962
Schnerder W and Seeger K 1966 *Appl. Phys. Lett.* **8** 133
- [31] Januszewski M and Łuczka J 2011 *Phys. Rev. E* **83** 051117
- [32] Januszewski M and Kostur M 2010 *Comput. Phys. Commun.* **181** 183
- [33] S. Ooi S, Savel'ev S, Gaifullin M B, Mochiku T, Hirata K and Nori F 2007 *Phys. Rev. Lett.* **99** 207003
- [34] Kostur M and Łuczka J 2001 *Phys. Rev. E* **63** 021101